

OVERVIEW OF THE MICROSCOPE OBJECTIVE

by

Ruijuan Niu

---

Copyright © Ruijuan Niu 2017

A Thesis Submitted to the Faculty of the

DEPARTMENT OF OPTICAL SCIENCES

In Partial Fulfillment of the Requirements

For the Degree of

MASTER OF SCIENCE

In the Graduate College

THE UNIVERSITY OF ARIZONA

2017

## STATEMENT BY AUTHOR

The thesis titled Overview of the Microscope Objective prepared by Ruijuan Niu has been submitted in partial fulfillment of requirements for a master's degree at the University of Arizona and is deposited in the University Library to be made available to borrowers under rules of the Library.

Brief quotations from this thesis are allowable without special permission, provided that an accurate acknowledgement of the source is made. Requests for permission for extended quotation from or reproduction of this manuscript in whole or in part may be granted by the head of the major department or the Dean of the Graduate College when in his or her judgment the proposed use of the material is in the interests of scholarship. In all other instances, however, permission must be obtained from the author.

SIGNED: Ruijuan Niu

## APPROVAL BY THESIS DIRECTOR

This thesis has been approved on the date shown below:

---

Jose M. Sasian  
Professor of Optical Sciences

04/26/2017  
Date

## ACKNOWLEDGMENTS

I would first like to thank my thesis advisor, Dr. Jose Sasian for providing guidance. I appreciate his kindness and support during these years. I would not be able to complete my thesis without his mentoring. I would like to acknowledge the members of my committee, Dr. Hong Hua and Dr. Yuzuru Takashima, who took their time to review this thesis and gave me valuable suggestions.

I would like to thank my parents and my grandmother for their support and encouragement throughout my years of study. I would also like to thank my best friends, Zinan, Jingyuan and Xiao, for caring about me even we are not in the same country. I thank my cats, Kili and Feifei, for being my family here in Tucson. I thank my boyfriend, Yuechen, for supporting me all the time.

## DEDICATION

To my grandfather, Liming Tang.

## TABLE OF CONTENTS

|  |    |
|--|----|
| LIST OF TABLES .....   | 7  |
| LIST OF FIGURES .....  | 8  |
| ABSTRACT .....   | 11 |
| CHAPTER 1. INTRODUCTION .....  | 12 |
| 1.1 The field of optical microscope lens objectives .....                            | 12 |
| 1.2 Goals of this thesis .....   | 14 |
| CHAPTER 2. MAIN CHARACTERISTICS OF MICROSCOPE OBJECTIVES .....                       | 15 |
| 2.1 Markings .....   | 15 |
| 2.1.1 Manufacturer .....   | 16 |
| 2.1.2 Objective Class .....  | 16 |
| 2.1.3 Magnification & numerical aperture (NA) .....                                  | 17 |
| 2.1.4 Contrast method .....  | 17 |
| 2.1.5 Immersion fluid .....  | 18 |
| 2.1.6 Tube length, cover glass thickness, working distance & correction collar ..... | 18 |
| 2.2 Magnification .....  | 19 |
| 2.3 Resolution & numerical aperture (NA) .....                                       | 20 |
| 2.4 Working distance .....   | 21 |
| 2.5 Entrance pupil and exit pupil location .....                                     | 21 |
| 2.6 Cover glass .....  | 21 |
| 2.7 Immersion .....  | 21 |
| 2.8 Contrast enhancing .....   | 22 |
| 2.8.1 Bright field .....   | 23 |
| 2.8.2 Dark field .....   | 24 |
| 2.8.3 Polarization .....   | 24 |
| 2.9 Tube length .....  | 26 |
| 2.10 Type of objectives .....  | 27 |
| 2.10.1 Reflective objective .....  | 27 |

TABLE OF CONTENTS—*Continued*

|   |    |
|---|----|
| 2.10.2 Refractive objective .....                     | 28 |
| 2.10.2.1 Achromatic objective .....                   | 29 |
| 2.10.2.2 Fluorite (semi-apochromatic) objective ..... | 30 |
| 2.10.2.3 Apochromatic objective .....                 | 30 |
| 2.11 Image quality .....                              | 31 |
| 2.12 Mechanical dimensions.....                       | 31 |
| 2.13 Vendors .....                                    | 32 |
| CHAPTER 3. FIRST ORDER MODELING OF AN OBJECTIVE ..... | 33 |
| 3.1 Paraxial surface thin lens model .....            | 34 |
| 3.2 Standard surface thin lens model .....            | 38 |
| 3.3 Thin lens with principal plane model.....         | 41 |
| 3.4 Conclusion .....                                  | 44 |
| CHAPTER 4 DESIGN EXAMPLES.....                        | 46 |
| 4.1 Achromatic objective .....                        | 46 |
| CHAPTER 5 CONCLUSION.....                             | 59 |
| REFERENCES .....                                      | 60 |

## LIST OF TABLES

|   |    |
|---|----|
| Table 1 aberration correction vs abbreviation .....                                 | 16 |
| Table 2 Magnification of eyepiece, objective and microscope.....                    | 19 |
| Table 3 Objective magnification and working distance .....                          | 21 |
| Table 4 The refractive indices of immersions.....                                   | 22 |
| Table 5 Objective type vs optical aberration correction .....                       | 28 |
| Table. 6 Comparison of 3 first order models .....                                   | 45 |
| Table. 7 Comparison of three achromatic objective models.....                       | 55 |
| Table 8 Comparison between the actual achromat model and the first order model..... | 58 |

## LIST OF FIGURES

|  |    |
|--|----|
| Figure 1.1 First microscope made by Hans and Zaccharias Janssen in 1590s .....     | 12 |
| Figure 1.2 Microscope made by Anton van Leeuwenhoek in 1675 .....                  | 13 |
| Figure 2.1 Objective Markings of a 60x Plan Apochromat Objective .....             | 15 |
| Figure 2.2 color coding of magnification .....                                     | 17 |
| Figure 2.3 Color of writing vs contrast method in Zeiss objectives .....           | 18 |
| Figure 2.4 color coding of immersion fluid .....                                   | 18 |
| Figure 2.5 Contrast-enhancing technologies in optical microscopy .....             | 23 |
| Figure 2.6 Dark field microscope optical configurations .....                      | 24 |
| Figure 2.7 polarizing light microscope optical pathways .....                      | 25 |
| Figure 2.8 Finite & infinity microscope optical system .....                       | 26 |
| Figure 2.9 Schwarzschild objective .....   | 27 |
| Figure 2.10 Chromatic aberration of a single lens .....                            | 29 |
| Figure 2.11 Chromatic aberration correction of an achromat .....                   | 29 |
| Figure 2.12 Chromatic aberration correction of an apochromatic objective .....     | 30 |
| Figure 2.13 Mechanical dimensions for a Zeiss plan-apochromat objective .....      | 32 |
| Figure 3.1 Lay out of the paraxial surface thin lens model .....                   | 34 |
| Figure 3.2 Lens data and system data of the paraxial surface thin lens model ..... | 35 |
| Figure 3.3 Aberration Seidel Diagram of the paraxial surface thin lens model ..... | 36 |
| Figure 3.4 Sketch of the objective in the paraxial surface thin lens model .....   | 36 |
| Figure 3.5 Sketch of the objective in the standard thin lens model .....           | 37 |
| Figure 3.6 Layout of the standard surface thin lens model .....                    | 38 |

## LIST OF FIGURES – *Continued*

|   |    |
|---|----|
| Figure 3.7 Lens data and system data of the standard surface thin lens model .....  | 39 |
| Figure 3.8 Aberration Seidel Diagram of the standard surface thin lens model.....   | 40 |
| Figure 3.9 Principal planes detail (Chief and Marginal ray only) .....              | 41 |
| Figure 3.10 Lay out of thin lens with principal plane model.....                    | 42 |
| Figure 3.11 Lens data and system data of thin lens with principal plane model ..... | 43 |
| Figure 3.12 Aberration Seidel diagram of thin lens with principal plane model.....  | 44 |
| Figure 4.1 Lens data of the achromat (a) .....                                      | 47 |
| Figure 4.2 System data of the achromat (a) .....                                    | 48 |
| Figure 4.3 Layout of the achromat (a) .....   | 48 |
| Figure 4.4 The chromatic focal shift of the achromat (a) .....                      | 49 |
| Figure 4.5 Seidel diagram of the achromat (a) .....                                 | 49 |
| Figure 4.6 Merit function of the achromat (a) .....                                 | 50 |
| Figure 4.7 The chromatic focal shift of the achromat (b) .....                      | 50 |
| Figure 4.8 Seidel diagram of the achromat (b).....                                  | 51 |
| Figure 4.9 System data of the achromat (b) .....                                    | 51 |
| Figure 4.10 Layout of the achromat (c) .....  | 52 |
| Figure 4.11 Lens data of the achromat (c) .....                                     | 52 |
| Figure 4.12 Focal shift of the achromat (c) .....                                   | 53 |
| Figure 4.13 Seidel diagram of the achromat (c) .....                                | 53 |
| Figure 4.14 System data of the achromat (c) .....                                   | 54 |
| Figure 4.15 Cardinal points data of achromat (c) .....                              | 56 |

LIST OF FIGURES – *Continued*

|   |    |
|---|----|
| Figure 4.16 Lens data of the converted first order model for achromat (c) .....   | 56 |
| Figure 4.17 Layout of the converted first order model for achromat (c) .....      | 57 |
| Figure 4.18 System data of the converted first order model for achromat (c) ..... | 57 |

## ABSTRACT

Microscopes are widely used in research and industry. The objective lens is the most significant part of the microscope. Some characteristics and different types of microscope objectives are discussed in this thesis. The markings on the objective indicate some main optical characteristics. However, it is not always possible to know the materials, the radius or the thickness of each surface in an objective lens and it is not easy to simulate an objective without this data. In this thesis, we build a first order model which can simulate a refractive microscope objective when the magnification and numerical aperture are known. The model contains a thin lens made by two standard surfaces and also simulates the principal planes. This model provides more accurate ray heights and it is aplanatic. Some design examples of an objective lens are also discussed in order to get a better understanding of design and optimization considerations.

## CHAPTER 1. INTRODUCTION

### 1.1 The field of optical microscope lens objectives

Humans have always wanted to explore the unknown world since the beginning of history <sup>[1]</sup>. Roman people knew glass during 1<sup>st</sup> century AD. However, aberration correcting lenses were not widely used until spectacles were made in Italy at the end of the 13<sup>th</sup> century. The early “microscope” only contained magnifying glasses which had one power about 6x-10x. This kind of microscope was called “flea glasses” since it was used to look at some small insects like fleas. In the 1590s, two Dutch spectacle makers, Hans and Zacharias Janssen, created the first microscope, which was described as “composed of 3 sliding tubes, measuring 18 inches long when fully extended, and two inches in diameter” (shown in Figure 1.1). It had a magnification from 3x to 9x.



Figure 1.1 First microscope made by Hans and Zaccharias Janssen in 1590s.

Later in 1675, a Dutch draper and scientist, Antony Van Leeuwenhoek made himself a microscope with a power of 270x and observed bacteria (shown in Figure 1.2).

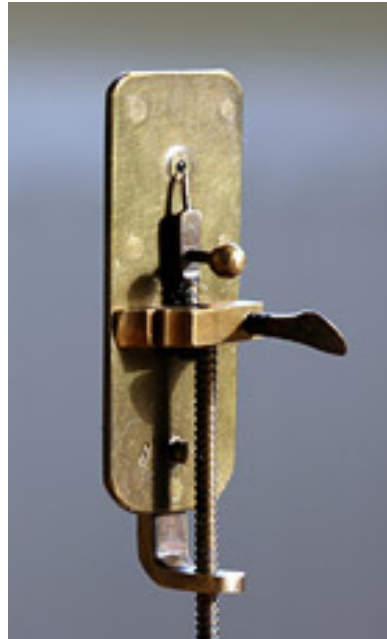


Figure 1.2 Microscope made by Anton van Leeuwenhoek in 1675.

With the study of optical principles, microscopes were improved rapidly from the middle of the 19<sup>th</sup> century to the 20<sup>th</sup> century. Recently, as the optical limits have been reached and the development of novel microscopes has slowed, more efforts are put into vision engineering to produce a user-friendly microscope.

A microscope is made not only to observe small objects in detail but also to give visibility to some tiny objects which may otherwise be invisible or unknown to us. The objective lens is one of the most significant parts among all the optical components in the microscope. When we use a microscope, the objective is at the nearest place from the object and forms an intermediate image, which can be magnified by eyepieces and produce a magnified image for people to observe. The objective lens determines how small of an object can be seen clearly through the microscope.

## **1.2 Goals of this thesis**

This thesis includes two parts. The first part is an overview of microscope objectives, which discusses optical characteristics of microscope objectives and different types of objectives. The second part is a first order model of an objective, and some designs for an achromatic objective. The goals of these two parts are 1) to provide a brief overview of microscope objective technology and terms used in characterizing an objective, 2) to introduce a useful model to simulate first-order layouts of microscope objectives, 3) to illustrate some steps in the design and optimization of a microscope objective.

Many figures in this thesis are taken from the open literature and are acknowledged in the references section.

## CHAPTER 2. MAIN CHARACTERISTICS OF MICROSCOPE OBJECTIVES

In this chapter, some main characteristics of the microscope objectives are introduced to 1) understand the meaning of an objective's markings, 2) have a brief overview of different characteristics of microscope objectives and microscopy technology.

### 2.1 Markings

Markings are usually printed outside of the objective. Some basic optical and mechanical specifications are indicated by words, numbers or colors. A 60x plan apochromatic objective shown in Figure 2.1 will be discussed as an example <sup>[2]</sup>.



Figure 2.1 Objective Markings of a 60x Plan Apochromat Objective.

### 2.1.1 Manufacturer

Usually the manufacturer name will be written in the first line. Nikon is the manufacturer in Figure 2.1.

### 2.1.2 Objective Class

The second line shows the type of the objective. The objective is a plan apochromatic objective, which corrects flat-field and aberration. Some corrections and their abbreviations are in Table 1.

Table 1 aberration correction vs abbreviation.

| <b>Abbreviation</b>                 | <b>Type</b>                                   |
|-------------------------------------|---|
| Achro, Achromat                     | Achromatic aberration correction              |
| Fluor, Fl, Fluor, Neofluor, Fluotar | Fluorite aberration correction                |
| Apo                                 | Apochromatic aberration correction            |
| Plan, Pl, Achroplan                 | Flat Field optical correction                 |
| EF, Acroplan                        | Extended Field (field of view less than Plan) |
| N, NPL                              | Normal field of view plan                     |
| Plan Apo                            | Apochromatic and Flat Field correction        |

### 2.1.3 Magnification & numerical aperture (NA)

Magnification and numerical aperture (NA) are in the third line. This objective has a magnification of 60x and an NA of 0.95. Manufacturers always paint a colored circle which follows a color coding (shown in Figure 2.2) on the objective in order to estimate the magnification of an objective. The blue circle in Figure 2.1 shows that the magnification is between 40 to 63. Users can easily pull out the objective they want among a lot of different objectives based on the color coding <sup>[3]</sup>.

#### Color Coding of Magnification:










|             |  |
|-------------|--|
| 1.0/1.25    |    |
| 2.5         |   |
| 4/5         |  |
| 6.3         |  |
| 10          |  |
| 16/20/25/32 |  |
| 40/50       |  |
| 63          |  |
| 100/150     |  |

Figure 2.2 color coding of magnification.

### 2.1.4 Contrast method

DIC (differential interference contrast) which is listed under the magnification, shows the contrast method of the objective. Sometimes the writing color of the markings also gives

the contrast method. For example, Zeiss makes its objectives markings written in different colors to distinguish the contrast method (shown in Figure 2.3).

|            |  |
|------------|--|
| Standard   |  |
| Pol/DIC    |  |
| Ph 0 1 2 3 |  |

Figure 2.3 Color of writing vs contrast method in Zeiss objectives.

### 2.1.5 Immersion fluid

Immersion fluid is used between object and the objective to enlarge NA and get a better-quality image. Immersion is usually printed after contrast method and follows the color coding of immersion fluid (Figure 2.4).





|                    |  |
|--------------------|--|
| Immersion Fluid:   |  |
| Oil                |  |
| Water              |  |
| Glycerin           |  |
| Oil/Water/Glycerin |  |

Figure 2.4 color coding of immersion fluid.

### 2.1.6 Tube length, cover glass thickness, working distance & correction collar

The tube length, cover glass thickness, working distance & correction collar specifications are in the fourth line. The tube length of the objective indicates whether it is finite conjugate or not, and the focal length of the objective if it is. In this case, the

objective is infinite conjugate hence the tube length is infinite. Cover glass thickness is between 0.11 mm -0.23 mm. The standard cover glass thickness is 0.17 mm. WD, (i.e. working distance) is 0.15 mm. Most objectives can adjust themselves by adjusting the correction collar to work with different cover glass thickness.

More details about these specifications are introduced later in this thesis in order to understand the markings.

## 2.2 Magnification

One of the most important characteristics is magnification. The magnification of a microscope is the product of the magnifications in the objective and the eyepiece <sup>[4]</sup>, shown in Table 2.

Table 2 Magnification of eyepiece, objective and microscope.

| <b>Eyepiece</b> | <b>Objective Lens</b> | <b>Total Magnification</b> |
|-----------------|-----------------------|----------------------------|
| 10X             | 4X                    | 40X                        |
| 10X             | 10X                   | 100X                       |
| 10X             | 40X                   | 400X                       |
| 10X             | 100X                  | 1000X                      |

With the same eyepiece, the larger the objective magnification is, the larger the microscope magnification will be. Magnification of an objective can range from 1x - 250x.

### **2.3 Resolution and numerical aperture (NA)**

Resolution determines the ability of the objective to detect fine detail. There are three design characteristics of the objectives in order to set the resolution limit of the microscope: wavelength of object illumination light, refractive index in the object space and angular aperture of the light cone captured by the objective. In the diffraction-limited optical microscope, resolution is the minimum visible distance  $r$  between the two closest separate object points <sup>[5]</sup>. The relationship between wavelength, refractive index, insert light angle and resolution is shown in equation 1.

$$r = \lambda / 2n \sin U \quad (1),$$

In Eq. 1,  $r$  is the resolution,  $\lambda$  is the wavelength of insert light,  $n$  is the refractive index in the object space,  $U$  is the half angle of the light cone.

Eq. 1 can be written in a simpler way with the definition of numerical aperture (shown in Eq. 2).

$$\text{Numerical Aperture (NA)} = n \sin U \quad (2),$$

Hence the Eq. 1 can be rewritten as

$$r = \lambda / (2 \text{ NA}) \quad (3),$$

A high NA is preferred in the objective to obtain a decent resolution.

## 2.4 Working distance

Working distance is the distance between the top of the cover glass or the object and the front surface of the objective front lens <sup>[6]</sup>. Working distance usually decreases as magnification increases, shown in Table 3.

Table 3 Objective magnification and working distance.

| Property                | Objective |           |            |               |
|-------------------------|-----------|-----------|------------|---------------|
|                         | Scanning  | Low Power | High Power | Oil Immersion |
| <b>Magnification</b>    | 4X        | 10X       | 40-45X     | 90-100X       |
| <b>Working distance</b> | 17-20 mm  | 4-8 mm    | 0.5-0.7 mm | 0.1mm         |

## 2.5 Entrance pupil and exit pupil location

Microscope objective is telecentric in object space, hence the entrance pupil is at infinity in image space and the exit pupil is at the front surface of the objective.

## 2.6 Cover glass

A proper cover glass can affect the image quality, especially for a high NA objective.

## 2.7 Immersion

Generally, there are three types of immersion: water, oil and glycerin. The refractive indices of immersions are different (Table 4) to achieve different NAs.

Table 4 The refractive indices of immersions.

| <b>Material</b>  | <b>Refractive Index</b> |
|------------------|-------------------------|
| Air              | 1.0003                  |
| Water            | 1.333                   |
| Glycerin         | 1.4695                  |
| Paraffin oil     | 1.480                   |
| Cedar wood oil   | 1.515                   |
| Synthetic oil    | 1.515                   |
| Anisole          | 1.5178                  |
| Bromonaphthalene | 1.6585                  |
| Methylene iodide | 1.740                   |

## **2.8 Contrast enhancing**

Sometimes the object or specimen cannot be observed easily due to its low contrast quality. Different methods are used to enhance the contrast, such as bright field, dark field, polarization, phase contrast, differential interference contrast (DIC) and Hoffman

modulation <sup>[7]</sup>. Some examples are shown in Figure 2.5. Bright field, dark field and polarization are briefly introduced in this part.

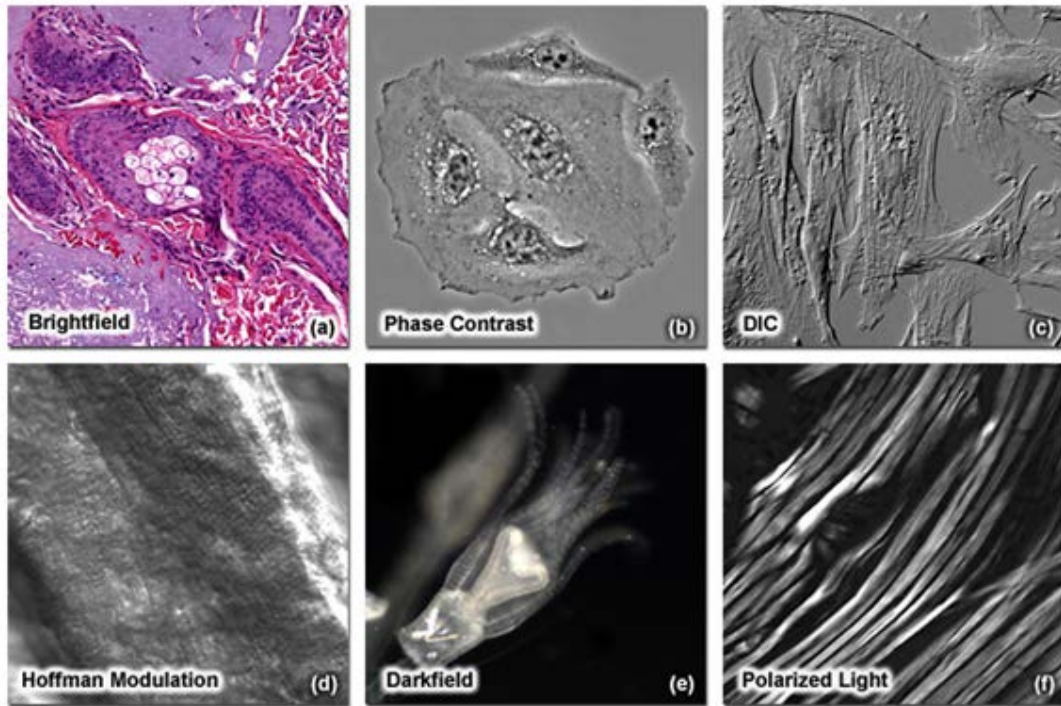


Figure 2.5 Contrast-enhancing technologies in optical microscopy.

### 2.8.1 Bright field

Bright field, as its name indicates, is putting the incident light source under the object and condenser. Bright field is one of the primary and most common used techniques since the microscope was invented. It depends on refractive index, light absorption changes and color for generating contrast. Therefore, bright field is not suitable for unstained transparent objects. The numerical aperture of both the object and the condenser can affect the resolution in a bright field system.

### 2.8.2 Dark field

As for unstained transparent objects, the image will be bright and low-contrast if bright field is applied in the system. Adding a dark field patch stop between the incident light source and the condenser is the dark field illumination. The image is composed mostly of diffracted wave (shown in Figure 2.6). Dark field illumination is widely used in biological and medical fields.

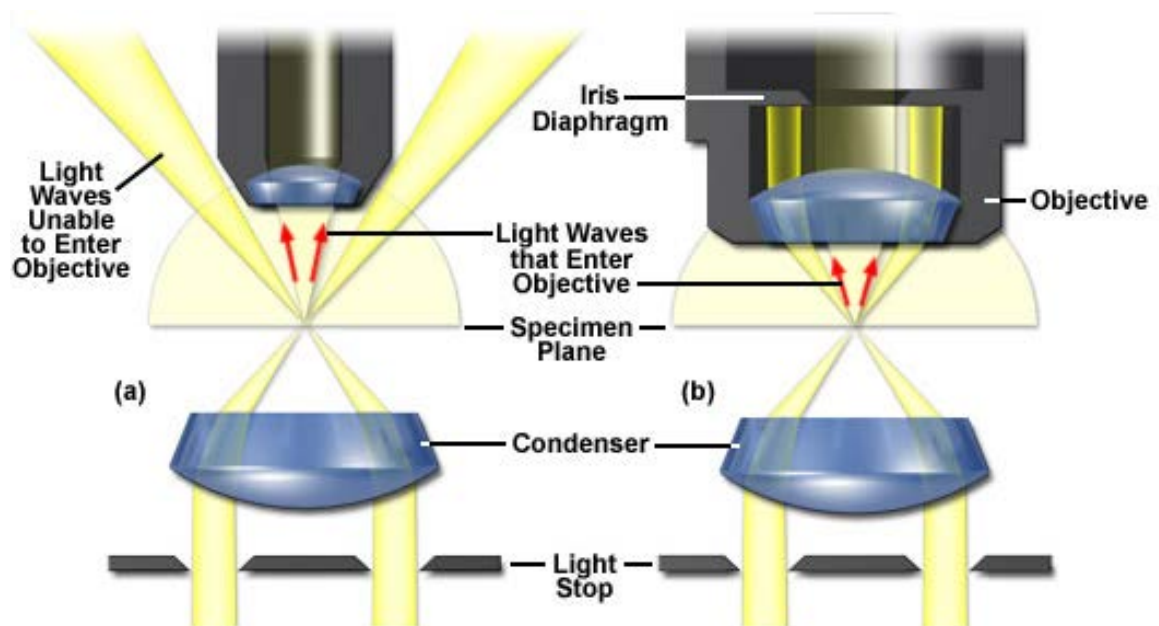


Figure 2.6 Dark field microscope optical configurations.

### 2.8.3 Polarization

If the object is anisotropic, such as crystals, for which the refractive index depends on the vibration direction of the incident light, polarized light can improve the image quality dramatically. Two polarizing elements are placed in this method (Figure 2.7).

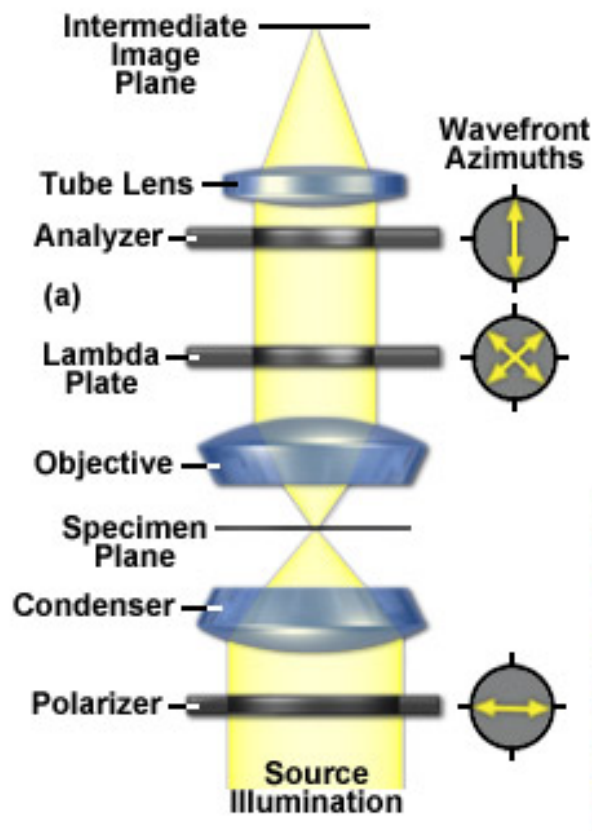


Figure 2.7 polarizing light microscope optical pathways.

The polarizer between the incident light source and the condenser makes linear polarized wavefront pass through the condenser and illuminate the object. The polarizer beneath the tube lens (analyzer) is rotated 90 degrees around the other polarizer. If there is no object, there will be no light passing through the tube lens. If an anisotropic object is placed, it will have different refractive indices when the light passes through. There is an optical path difference between the two wavefronts. Therefore, when the analyzer combines the two wavefronts again, the two wavefronts will have the same amplitude at the time of maximum contrast.

## 2.9 Tube length

If the tube length of an objective is finite, it is a finite optical system (shown in Figure 2.8 (a)). If the tube length of an objective is infinite, it is infinitely corrected and an infinite objective needs a tube lens between it and the eyepiece (shown in Figure 2.8 (b)).

Most available objectives now are infinite.

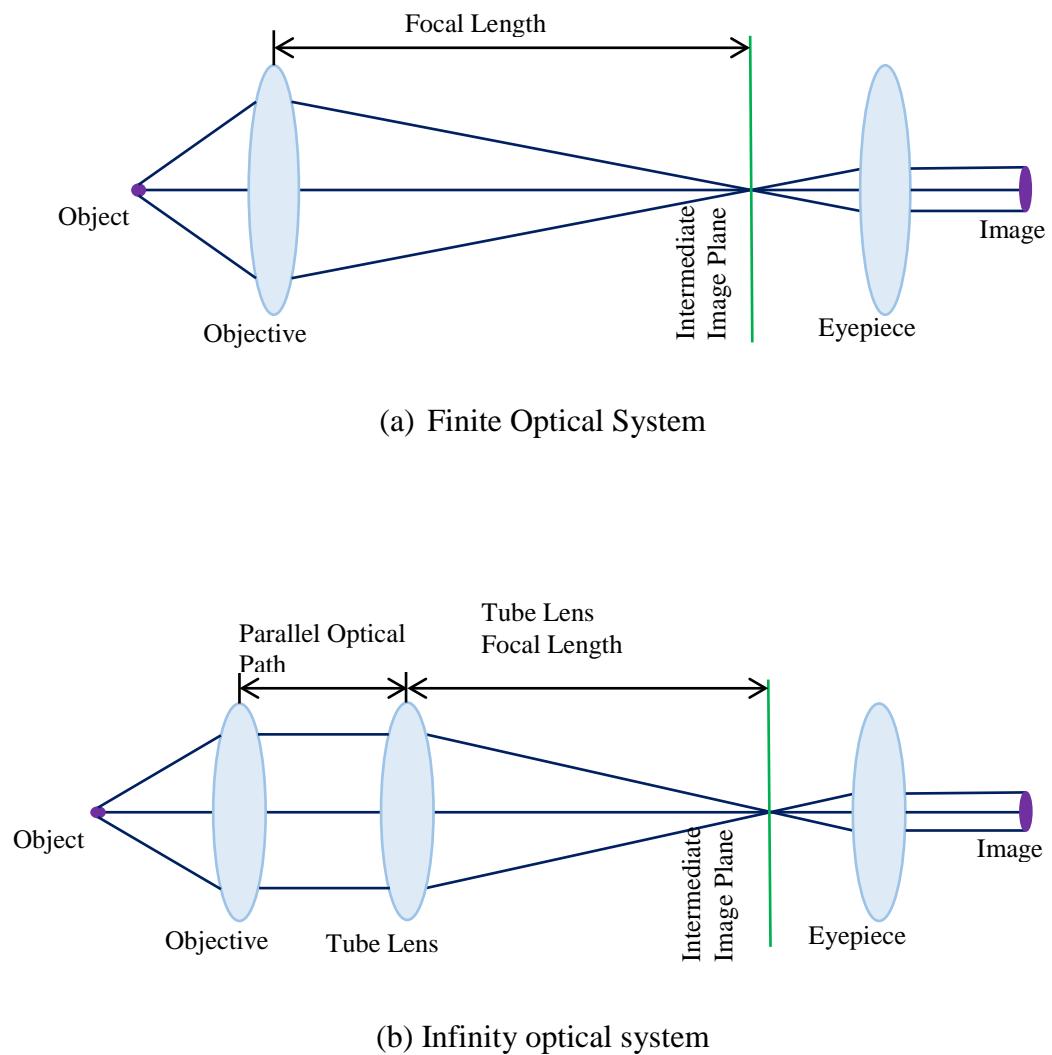


Figure 2.8 Finite & infinity microscope optical system.

## 2.10 Type of objectives

Objectives have 2 main different types: refractive and reflective.

### 2.10.1 Reflective objective

The incident light passes through the optical system refracted by a series of optical lenses in refractive objectives. All elements are coated to reduce reflections and increase light throughout the rate. Reflective objectives are made to get high magnification and correct chromatic aberration from deep-ultraviolet to far-infrared light. Reflective objectives are mostly mirror-based designs. The most used type is two-mirror Schwarzschild objective (shown in Figure 2.9), which has a spider mount and two mirrors covered with coatings.

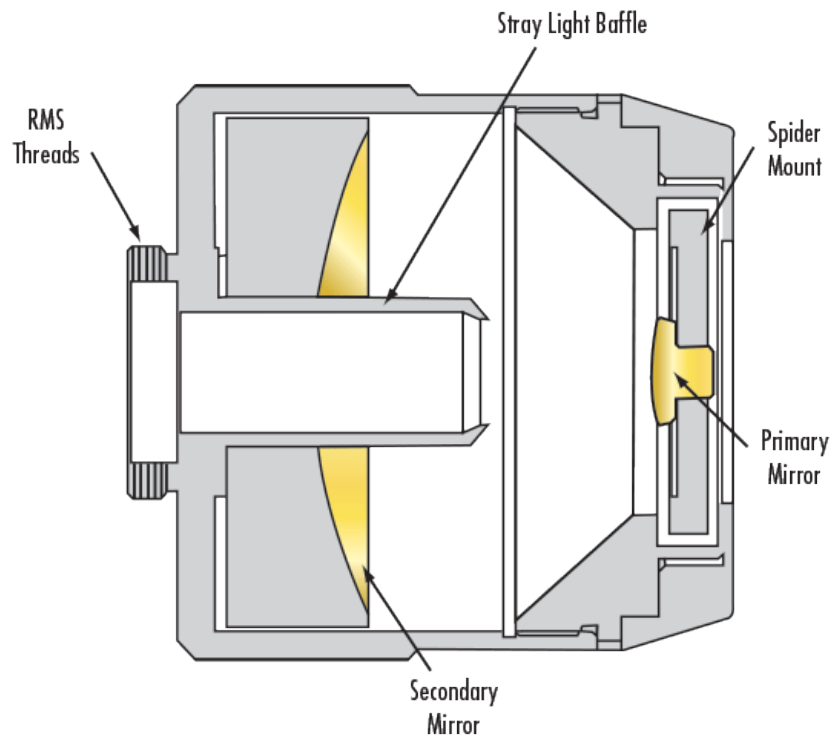


Figure 2.9 Schwarzschild objective.

### 2.10.2 Refractive objective

Most traditional microscopes use refractive objectives. There are different types of refractive objectives: achromatic, fluorite (semi-apochromatic), apochromatic and plan objectives. Each type has different aberration corrections (shown in Table 5).

Table 5 Objective type vs optical aberration correction.

| <b>Objective Type</b>  | <b>Spherical Aberration</b> | <b>Chromatic Aberration</b> | <b>Field Curvature</b> |
|------------------------|-----------------------------|-----------------------------|------------------------|
| <b>Achromat</b>        | 1 color                     | 2 colors                    | No                     |
| <b>Plan Achromat</b>   | 1 color                     | 2 colors                    | Yes                    |
| <b>Fluorite</b>        | 2-3 colors                  | 2-3 colors                  | No                     |
| <b>Plan Fluorite</b>   | 3-4 colors                  | 2-4 colors                  | Yes                    |
| <b>Plan Apochromat</b> | 3-4 colors                  | 4-5 colors                  | Yes                    |

The chromatic aberration correction is one of the most important aberration corrections in the objectives. The material index is different due to the wavelength difference for the non-monochromatic light. Therefore, the focal length is not the same for different color.

The chromatic aberration of a single lens is shown in Figure 2.10.

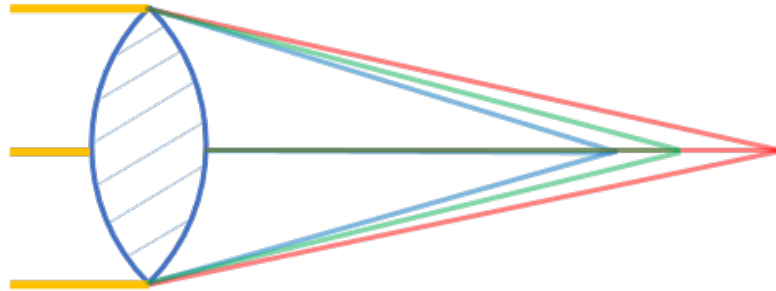


Figure 2.10 Chromatic aberration of a single lens.

The achromat lens is the simplest way for the objective to correct some aberrations.

### 2.10.2.1 Achromatic objective

The most common and least expensive refractive objectives are achromatic objectives (achromat). These objectives are made to correct axial chromatic aberration in two wavelengths, usually blue (486 nm) and red (656 nm), and cancel the distance between each focal point (shown in Figure 2.11).

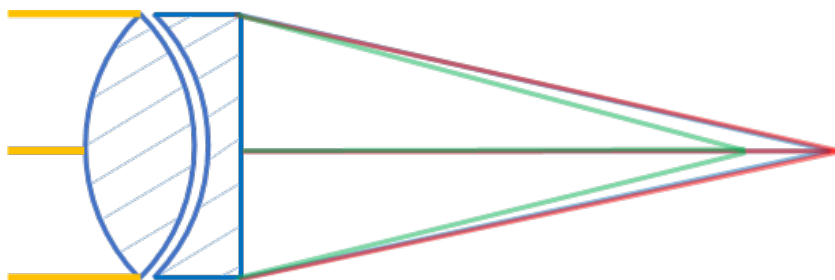


Figure 2.11 Chromatic aberration correction of an achromat.

Furthermore, the achromatic objective corrects spherical aberration for green light (546 nm), hence a green filter (interference filter) can be used to get a better image. The center of the achromatic objective is focused, but the edge of the objective may not be. For most

purposes, it can produce an adequate result, when objective requires focused lens periphery (i.e. correct field curvature), plan achromatic objective is needed.

### 2.10.2.2 Fluorite (semi-apochromatic) objective

The second type of objective is fluorite or semi-apochromatic, which was used for mineral fluorite. Fluorite objectives not only correct axial chromatic aberration in blue and red lights, but also provide spherical aberration correction for two or three colors.

Fluorite objectives have better resolution and higher NAs compare to achromatic objectives, hence they are more expensive as well. They are widely used for fluorescence observation. Plan fluorites are also made to correct field curvature.

### 2.10.2.3 Apochromatic objective

The third type is apochromatic objectives, which are the most expensive and highly corrected among these three types of objectives. Apochromatic objectives are corrected chromatically for three colors (red, green and blue) (shown in Figure 2.12), and provide spherical aberration correction for two or three colors as are fluorites.

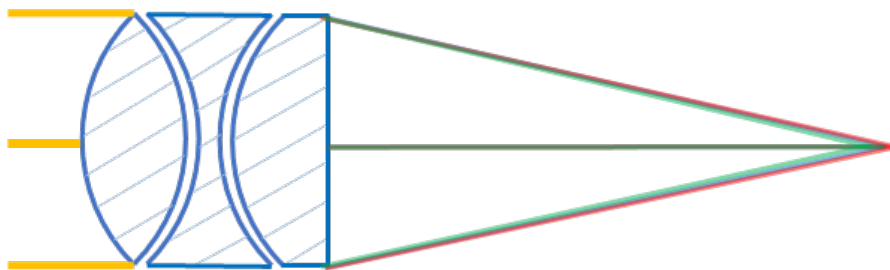


Figure 2.12 Chromatic aberration correction of an apochromatic objective.

Apochromatic objectives can be used for color photomicrography in white light because they almost eliminate chromatic aberration and have higher numerical aperture for the same magnification compared to achromatic and fluorite objectives. Plan apochromatic objectives are the most complex and expensive objectives which correct chromatic aberration and field curvature within the objective itself.

### **2.11 Image quality**

The image provided by the microscope needs to be as accurate as possible with aberration (spherical and chromatic aberration) and spurious detail removed. Most microscope objectives now are fully corrected and eyepieces or tube lenses are free from additional correction.

### **2.12 Mechanical dimensions**

The mechanical data sheet is needed to choose the correct objective for a microscope tube. It includes diameters and lengths of each part. Figure 2.13 is the mechanical dimensions of a Zeiss 40x plan-apochromat objective. The diameters, lengths and object plan can be found out easily in this figure.

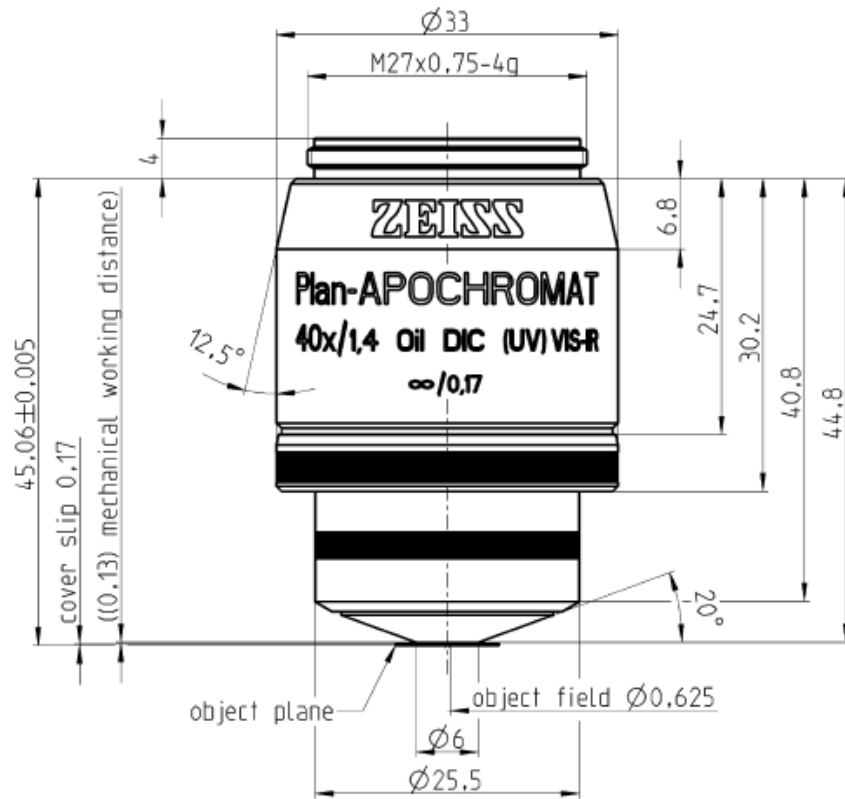


Figure 2.13 Mechanical dimensions for a Zeiss plan-apochromat objective.

### 2.13 Vendors:

There are many microscope objective vendors around the world. Some of the most famous ones are Zeiss, Nikon, Edmund, Olympus etc.

### CHAPTER 3. FIRST ORDER MODELING OF AN OBJECTIVE

In order to analyze a microscope, sometimes it is necessary to have a simple model for the objective lens. This is because the detailed specifications of a microscope objective are not always known; for instance, the surface radii, distances between surfaces and refraction indices may not be provided. In this chapter, three different and simple models for a microscope objective lens are discussed to get a better understanding of the microscope objective. Zemax Optics Studio lens design program is used to build the models to simulate the objective lens and system<sup>[8]</sup>. The infinity- corrected objective is chosen to be simulated, since it is widely used in industrial microscopes. The models have two parts, an objective and a tube lens. The object was placed at the front focal plane of the objective, so the light bundle was parallel after passing through the objective for one object point. An intermediate image was formed after the light went through the tube lens which was placed between the objective and the eyepiece. The intermediate image should be at the rear focal plane of the tube lens which is at a finite distance within the microscope tube. The infinity-corrected optical system is a telecentric system in object space. The magnifying power of this system is the focal length of the tube lens divided by the focal length of the objective.

The three models are a) paraxial surface in Zemax Optics Studio, b) standard surface, and c) standard surface with principal plane thin lens model. These models are used to simulate an objective which has the magnification of 20x and object space Numerical Aperture (NA) of 0.75. The objective has 5-mm focal length and the tube lens has 100-mm focal length in each model.

### 3.1 Paraxial surface thin lens model

Firstly, consider the objective and tube lens are two single thin lenses with 0 mm thickness. Assuming the system traces rays in very small heights and angles, it can follow the paraxial approximation (small-angle approximation). When angle  $\theta$  and  $\theta'$  are small enough ( $\theta < 0.2$  in radians) then there is Eq. 4.

$$\sin \theta \approx \theta,$$

$$\sin \theta' \approx \theta'. \quad (4)$$

For Snell's law,

$$n \sin \theta = n' \sin \theta', \quad (5)$$

can be approximated as

$$n \theta = n' \theta'. \quad (6)$$

The paraxial surface in Zemax Optics Studio can be used as the objective.

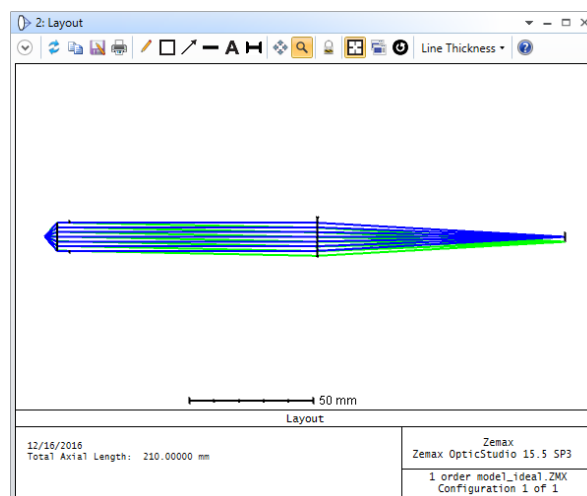


Figure 3.1 Lay out of the paraxial surface thin lens model.

The layout of this system is in Figure 3.1. Both objective and tube lens are paraxial thin lenses. The objective has 5 mm focal length and the object is placed at the front focal plane of this thin lens. The system stop is at the rear focal plane of the objective. The incident light passes through the objective and the intermediate image plane is at infinity. The tube lens is placed 100 mm behind the stop. The image is 100 mm behind the tube lens since the tube lens has 100 mm focal length. Both lens data and system data are listed in Figure 3.2. The paraxial image height is 2 mm when the object height is 0.1 mm, which achieved the magnification of 20x.

| Surf.Type         | Comment           | Radius   | Thickness | Material | Coating | Semi-Diameter | Chip Zone | Mech Semi | Conic  | Focal Length |
|-------------------|-------------------|----------|-----------|----------|---------|---------------|-----------|-----------|--------|--------------|
| 0 OBJECT Standard |                   | Infinity | 5.000     |          |         | 0.100         | 0.000     | 0.100     | 0.0... |              |
| 1 Paraxial        | objective         |          | 0.000     |          |         | 5.769         | -         | -         |        | 5.000        |
| 2 Standard        |                   | Infinity | 5.000     |          |         | 5.769         | 0.000     | 5.769     | 0.0... |              |
| 3 STOP Standard   | rear focal pla... | Infinity | 100.000   |          |         | 5.669         | 0.000     | 5.669     | 0.0... |              |
| 4 Paraxial        |                   |          | 100.000   |          |         | 7.669         | -         | -         |        | 100.000      |
| 5 IMAGE Standard  |                   | Infinity | -         |          |         | 2.000         | 0.000     | 2.000     | 0.0... |              |

```

Effective Focal Length :          1e+10    (in air at system temperature and pressure)
Effective Focal Length :          1e+10    (in image space)
Total Track             :              205
Image Space F/#         :          0.4409586
Paraxial Working F/#    :          8.819171
Working F/#             :          8.833333
Image Space NA          :          0.05660377
Object Space NA         :              0.75
Stop Radius             :          5.669467
Paraxial Image Height   :              2
Paraxial Magnification  :             -20
Entrance Pupil Diameter :          2.267787e+10
Entrance Pupil Position :              1e+10
Exit Pupil Diameter     :          1.133893e+09
Exit Pupil Position     :              1e+10
Field Type              :    Object height in Millimeters
Maximum Radial Field    :              0.1
Primary Wavelength [µm] :          0.5875618
Angular Magnification   :          -0.04999993

```

Figure 3.2 Lens data and system data of the paraxial surface thin lens model.

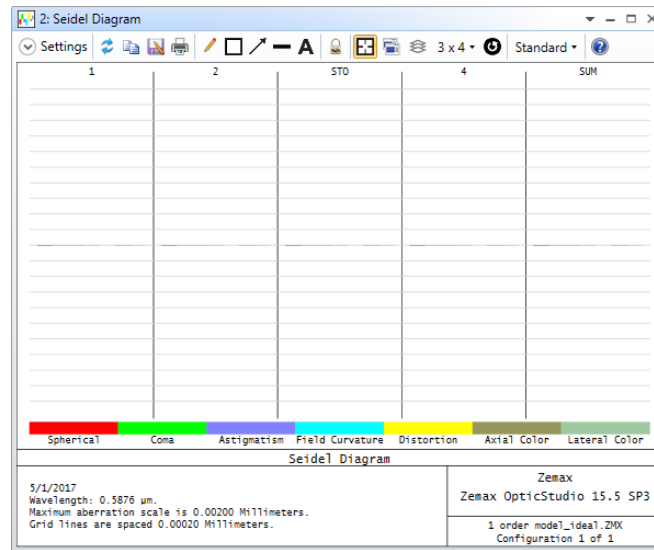


Figure 3.3 Aberration Seidel Diagram of the paraxial surface thin lens model.

There are no aberrations as shown in the Seidel diagram (shown in Figure 3.3), which is reasonable for a paraxial thin lens model. Realistically, an objective lens may have more aberrations, such as spherical aberration, field curvature and astigmatism. The model uses a paraxial surface as the thin lens, which is not suitable for the microscope objective. Also, this model is not ideal for us to discuss numerical aperture (NA).

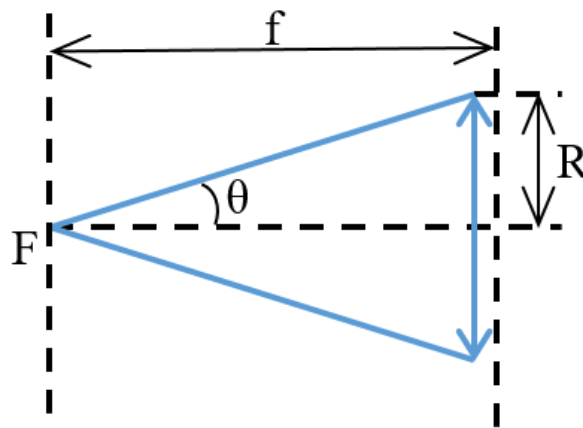


Figure 3.4 Sketch of the objective in the paraxial surface thin lens model.

From the system data, we noticed the stop radius is 5.669467 mm while object space  $NA = 0.75$  and  $f = 5$  mm. Obviously for the maximum half angle of the insert light,  $\theta$  (shown in Figure 3.4), with the small angle approximation,

$$\tan \theta = \text{stop radius} / f = 1.1338934. \quad (7)$$

$\theta = 48.59037741$  or  $0.84806207$  rad, indicates that NA cannot be assumed as  $n \theta$ . The object space NA is not accurate in this model. We can't use the paraxial thin lens because incident light angle is not small enough for paraxial ray-tracing. Another disadvantage of this model is that NA can't be calculated directly by the stop radius and the distance between the object and the objective.

To solve this problem, the paraxial surface can be replaced by the standard surfaces (shown in Figure 3.5). The first standard surface of the objective has radius curvature  $r = f$ , so that

$$NA = n \sin \theta = \text{stop radius} / r = \text{stop radius} / f. \quad (8)$$

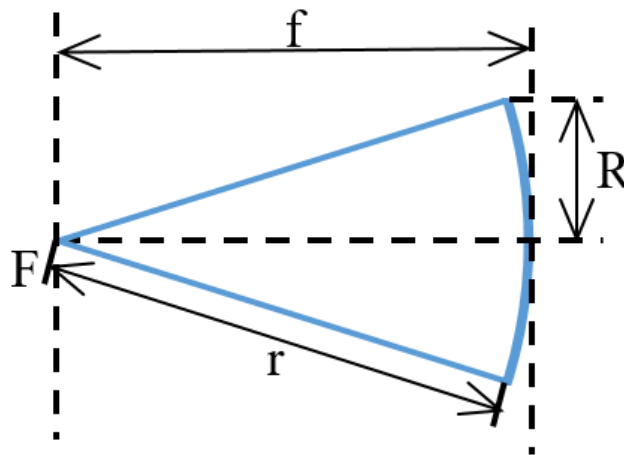


Figure 3.5 Sketch of the objective in the standard thin lens model.

### 3.2 Standard surface thin lens model

With the need of having a more accurate object space NA, the standard surface can be used in the system instead of the paraxial surface. In order to make a thin lens to be the objective, two or more standard surfaces are needed. Since this is a first order model, two standard surfaces are made to simulate the thin lens. The first surface has -5 mm radius so that the object is placed at the center point of the first standard surface as well as the front focal point of the thin lens. The objective space  $NA = n \sin \theta = \text{stop radius} / r = \text{stop radius} / f$ . The layout of the standard surface thin lens model is in Figure 3.6.

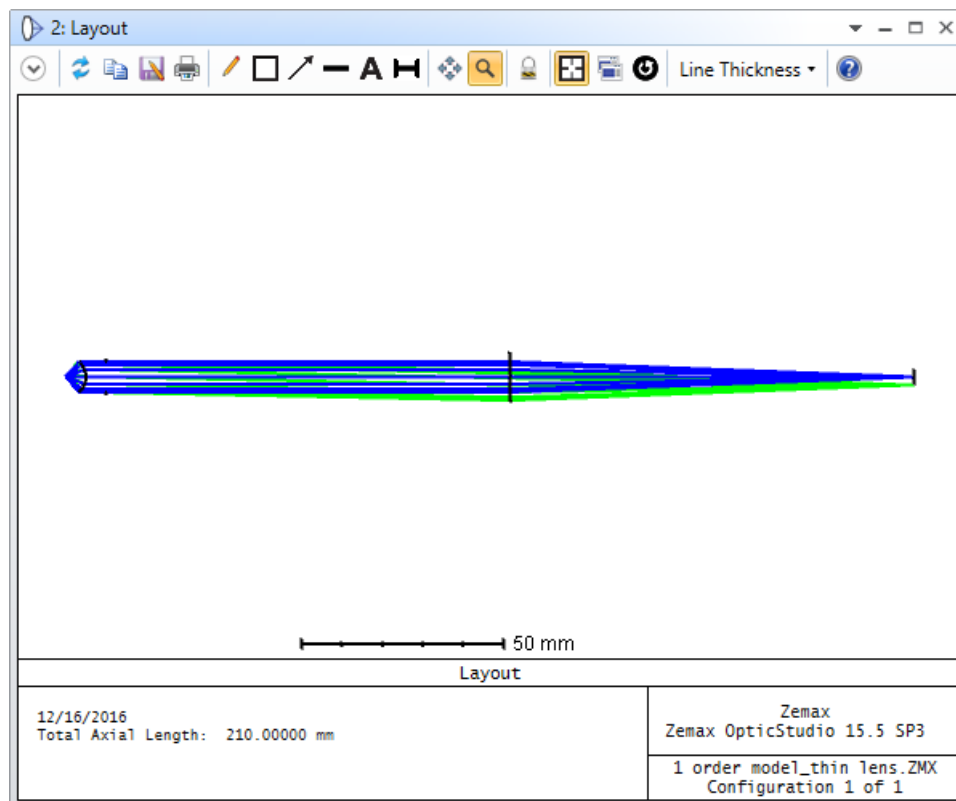


Figure 3.6 Layout of the standard surface thin lens model.

The lens data is listed in Figure 3.7.

|   | Surf>Type         | Comment                 | Radius   | Thickness | Material        | Coating | Semi-Diameter |
|---|-------------------|-------------------------|----------|-----------|-----------------|---------|---------------|
| 0 | OBJECT Standard ▾ |                         | Infinity | 5.000     |                 |         | 0.100         |
| 1 | Standard ▾        | objective front surface | -5.000   | 0.000     | -10000.00,0,0 V |         | 3.793         |
| 2 | Standard ▾        | objective back surface  | -5.000   | 5.000     |                 |         | 3.794         |
| 3 | STOP Standard ▾   | rear focal plane        | Infinity | 100.000   |                 |         | 3.836         |
| 4 | Paraxial ▾        | second lens             |          | 100.000   |                 |         | 5.789         |
| 5 | IMAGE Standard ▾  |                         | Infinity | -         |                 |         | 2.051         |

```

Effective Focal Length :          1e+10      (in air at system temperature and pressure)
Effective Focal Length :          1e+10      (in image space)
Back Focal Length      :          1.295872e+14
Total Track           :              205
Image Space F/#       :          0.4409586
Paraxial Working F/#  :          8.819171
Working F/#           :          13.34134
Image Space NA        :          0.05660377
Object Space NA       :          0.75
Stop Radius           :          5.669467
Paraxial Image Height :              2
Paraxial Magnification :             -20
Entrance Pupil Diameter :        2.267787e+10
Entrance Pupil Position :          1e+10
Exit Pupil Diameter   :          1.133893e+09
Exit Pupil Position   :          1e+10

```

Figure 3.7 Lens data and system data of the standard surface thin lens model.

The distance between the center of the two standard surfaces is 0 mm. The first surface has a radius of -5 mm, while the second surface has -5.0005 mm radius. Therefore, a thin lens is built, and since the focal length of the thin lens needs to be 5 mm, the index between the two surfaces should be variable to achieve the 5-mm focal length. The index between the two lenses is -10000.0000002 after optimized. Obviously, this index is not commonly used in an actual objective, but the high index allows the model to simulate an aplanatic lens. The equivalent refracting surface of an aplanat is spherical. The stop radius is 3.836 mm. If the equation  $NA = n \sin \theta = \text{stop radius} / r$  is used here, object space  $NA = 3.836 / 5 = 0.7672$ , which is very close to the desired value of  $NA = 0.75$ . The focal

length is the distance between the focal point and the principal point according to Gaussian optics.

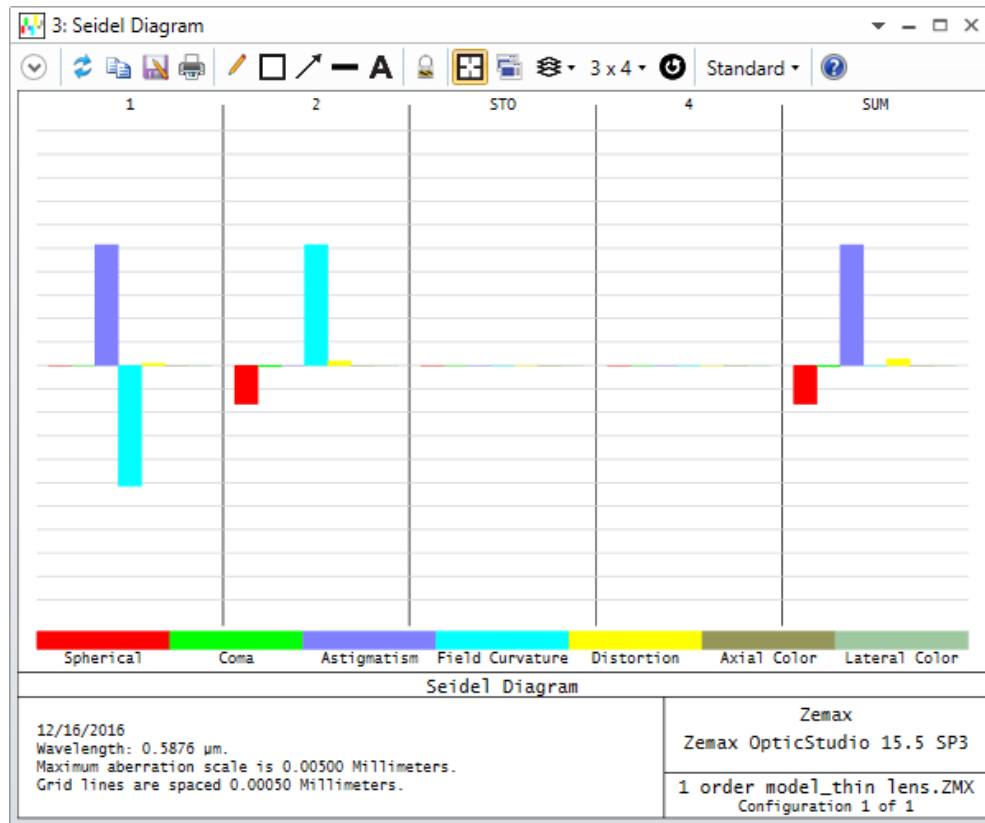


Figure 3.8 Aberration Seidel Diagram of the standard surface thin lens model.

There is no coma and nearly zero spherical aberration by construction. It mainly has astigmatism, distortion as shown on the Seidel diagram in Figure 3.8.

Furthermore, the lenses with thickness are needed in the actual objective. The objects are placed at the focal plane. If an objective is simulated by a first order model, the principal planes must be added. The third model is introduced next in order include the principal plane separation.

### 3.3 Thin lens with principal plane model

Once the principal planes separation is known, the lens system can be simplified as a single lens with principal planes. If we use thick lenses in modelling, we may not easily find the principal plane to determine the place of the focal point and the object.

Therefore, the thin lens with principal plane model are built to simulate this objective.

A ray emerges from the lens and crosses the rear principal plane at the same height as the same ray appeared to cross the front principal plane. A relay lens set with the magnification of 1x can be used as the principal planes (shown in Figure 3.9).

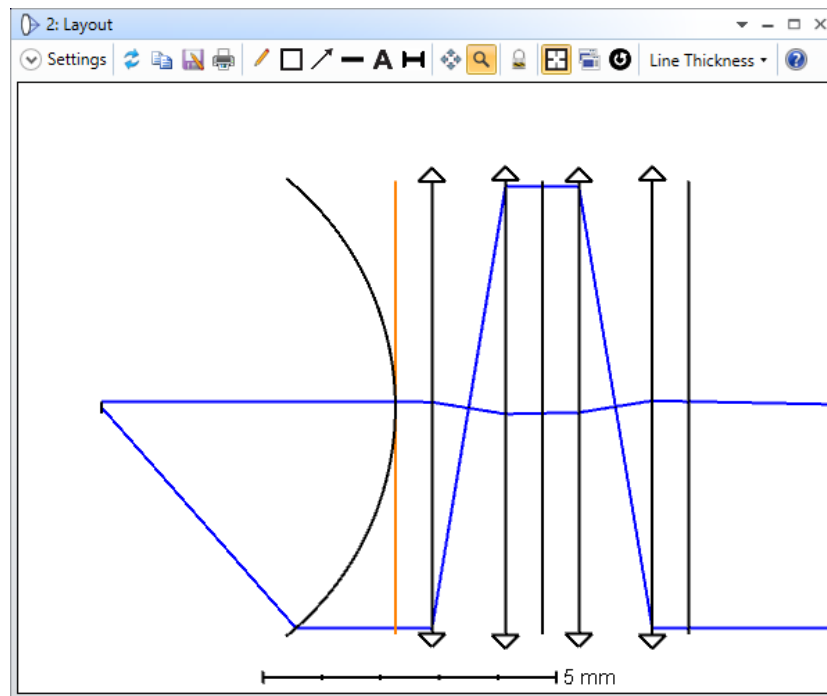


Figure 3.9 Principal planes detail (Chief and Marginal ray only).

The highlighted standard surface with infinity radius can be used as front principal plane. The last standard surface with infinity radius on the right is the rear principal

plane. Seven surfaces (including 4 paraxial thin lenses with  $-1\times$  magnification and 3 standard surfaces with infinity radius) are separated equally between two principal surfaces. When the parallel light bundles pass through the first paraxial thin lens, they focus on the rear focal point of the first paraxial thin lens as well as the front focal point of the second paraxial thin lens. Then the light bundles become parallel again with the opposite height. After passing through another same lens set, the light bundles are still parallel and have the same height as the highlight standard surface after they pass through the fourth paraxial thin lens and the last standard surface. A lay out of the whole system is clearer after hiding all the surfaces between two principal planes and the rays to these surfaces (shown in Figure 3.10).

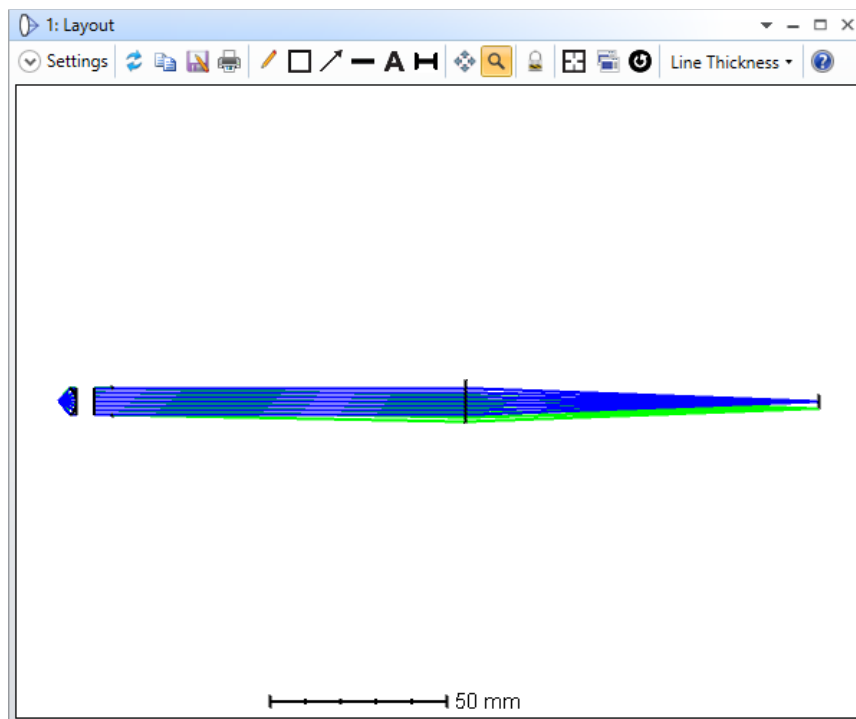


Figure 3.10 Lay out of thin lens with principal plane model.

The thicknesses of these surfaces can be set as pickup in Zemax, which are all equal to divide the distance between the two principal planes by 8. We set the distance to be 5 mm, so the thicknesses are 0.625 mm (shown in Figure 3.11). The index of lens material is positive, which is acceptable for the thin lens model. The ray heights in the model are also simulated properly. The stop radius is 3.75 mm. The object space NA= stop radius/focal length, or  $NA = 3.75 / 5 = 0.75$  in this case, which is the most accurate one among these three models.

|    | Surf>Type         | Comment       | Radius   | Thickness | Material      | Coating | Semi-Diameter | Chip Zone | Mech Semi-Dia | Conic |
|----|-------------------|---------------|----------|-----------|---------------|---------|---------------|-----------|---------------|-------|
| 0  | OBJECT Standard ▾ | Front Focal P | Infinity | 0.000     |               |         | 0.100         | 0.000     | 0.100         | 5.000 |
| 1  | Standard ▾        |               | Infinity | 5.000     |               |         | 0.100         | 0.000     | 0.100         | 0.000 |
| 2  | Standard ▾        | Objective     | -5.000   | 0.000     | 100000.00,0.0 |         | 3.891         | 0.000     | 3.891         | 0.000 |
| 3  | Standard ▾        | Objective     | -5.000   | 0.000     |               |         | 3.891         | 0.000     | 3.891         | 0.000 |
| 4  | Standard ▾        | Front PP      | Infinity | 0.625 P   |               |         | 3.853         | 0.000     | 3.853         | 0.000 |
| 5  | Paraxial ▾        |               |          | 0.625 P   |               |         | 3.840         | -         | -             |       |
| 6  | Standard ▾        |               | Infinity | 0.625 P   |               |         | 0.013         | 0.000     | 0.013         | 0.000 |
| 7  | Paraxial ▾        |               |          | 0.625 P   |               |         | 3.866         | -         | -             |       |
| 8  | Standard ▾        |               | Infinity | 0.625 P   |               |         | 3.853         | 0.000     | 3.853         | 0.000 |
| 9  | Paraxial ▾        |               |          | 0.625 P   |               |         | 3.840         | -         | -             |       |
| 10 | Standard ▾        |               | Infinity | 0.625 P   |               |         | 0.013         | 0.000     | 0.013         | 0.000 |
| 11 | Paraxial ▾        |               |          | 0.625 P   |               |         | 3.866         | -         | -             |       |
| 12 | Standard ▾        | Rear PP       | Infinity | 5.000     |               |         | 3.853         | 0.000     | 3.853         | 0.000 |
| 13 | STOP Standard ▾   | Rear Focal P  | Infinity | 100.000   |               |         | 3.750         | 0.000     | 3.750         | 0.000 |
| 14 | Paraxial ▾        | Second lens   |          | 100.000   |               |         | 5.700         | -         | -             |       |
| 15 | IMAGE Standard ▾  |               | Infinity | -         |               |         | 2.060         | 0.000     | 2.060         | 0.000 |

Effective Focal Length : -1.01495e+07 (in air at system temperature and pressure)  
 Effective Focal Length : -1.01495e+07 (in image space)  
 Back Focal Length : 2.029926e+08  
 Total Track : 215  
 Image Space F/# : 8.819231  
 Paraxial Working F/# : 8.819258  
 Working F/# : 13.34306  
 Image Space NA : 0.05660322  
 Object Space NA : 0.75  
 Stop Radius : -5.669411  
 Paraxial Image Height : 2.00002  
 Paraxial Magnification : -20.0002  
 Entrance Pupil Diameter : 1150838  
 Entrance Pupil Position : -507471.7  
 Exit Pupil Diameter : 7.499742e+08  
 Exit Pupil Position : 1e+10

Figure 3.11 Lens data and system data of thin lens with principal plane model.

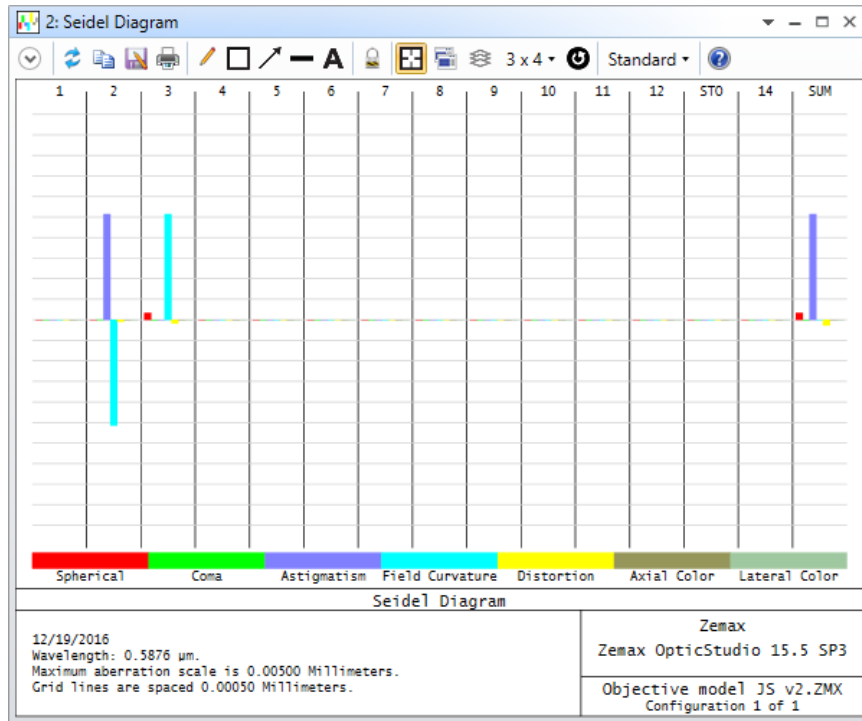


Figure 3.12 Aberration Seidel diagram of thin lens with principal plane model.

From the aberration Seidel diagram (shown in Figure 3.12), it is easy to figure out that the lens system mainly has astigmatism. The spherical aberration is quite small compared to the other two models, which is great to simulate an aplanatic objective.

### 3.4 Conclusion

The comparison of these 3 models is summarized in table 6:

Table. 6 Comparison of 3 first order models.

|                                       | <b>Advantages</b>  | <b>Disadvantages</b>  |
|---------------------------------------|--|---|
| <b>Paraxial thin lens</b>             | Easy to build<br><br>No aberration   | Non-accurate marginal ray<br><br>height and numerical aperture                        |
| <b>Standard surface thin lens</b>     | Easy to build  | No principal planes and does not simulate thick lens<br><br>Aplanatic by construction |
| <b>Thin lens with principal plane</b> | Accurate numerical aperture<br><br>Aplanatic as real objective<br><br>Easy to determine focal plane when simulating a thick lens | It uses several surfaces  |

The comparison in the Table 6 indicates that the thin lens with principal plane is the best first order model of simulating a microscope objective.

## CHAPTER 4. DESIGN EXAMPLES

Some design examples are discussed in this chapter to illustrate some steps in the design and optimization of a microscope objective.

### 4.1 Achromatic objective

In this section, an achromatic doublet is used as a finite conjugate achromatic objective.

A 4x/ 0.1 objective model is built. Set the optical tube length (OTL) as 170 mm, which means the image plane of this objective is at 170 mm behind the rear focal plane as well as the stop plane. The object is placed at the front focal plane of the objective in a microscope. The focal length of the objective follows equation 9:

$$f = d / M_o, \quad (9)$$

$f$  is the focal length of the objective,  $d$  is OTL,  $M_o$  is the magnification of the objective.

$$f = 170 / 4 = 42.5 \text{ mm}$$

However, the object plane is not easy to figure out in the model built in Zemax since the principal plane is not known in this optical system and the distance between the object and the first surface of the achromat is not accurate.

Therefore, the whole system can be flipped around in order to make the model clearer. The image plane of the objective can be set as the object plane.

It is obvious that the distance between the object and the stop is fixed as 170 mm. The stop should be at the front focal plane of this achromat and the location of the principal plane is unknown, so it is set to be a variable. The achromat is a doublet which contains a

2-mm thick concave lens (made of flint glass) and a 6-mm thick convex lens (made of crown glass). F2 and BK7 are chosen to be the materials of the achromat. Paraxial image height is chosen to be 1 mm in the field data to let the system be close to the objective with a 1-mm object. When NA is 0.1 for the objective, the image space NA is 0.1 in this system. The image space F/# is chosen as the aperture type, because:

$$F/\# \approx 1/(2 \text{ NA}), \quad (10)$$

The image space F/# =  $1/(2 \cdot 0.1) = 5$ . The lens data of the model is shown in Figure 4.1 after optimizing the system.

|   | Surf>Type         | Comment | Radius     | Thickness | Material | Coating | Clear Semi-Dia | Chip Zone | Mech Semi-Dia | Conic  | TCE x 1E-6 |
|---|-------------------|---------|------------|-----------|----------|---------|----------------|-----------|---------------|--------|------------|
| 0 | OBJECT Standard ▾ |         | Infinity   | 170.000   |          |         | 3.993          | 0.000     | 3.993         | 0.0... | 0.000      |
| 1 | STOP Standard ▾   |         | Infinity   | 42.327 V  |          |         | 4.254          | 0.000     | 4.254         | 0.0... | 0.000      |
| 2 | (aper) Standard ▾ |         | 20.132 V   | 2.000     | N-F2     | TH...   | 8.000 U        | 0.000     | 8.000         | 0.0... | -          |
| 3 | (aper) Standard ▾ |         | 10.243 V   | 6.000     | N-BK7    |         | 8.000 U        | 0.000     | 8.000         | 0.0... | -          |
| 4 | (aper) Standard ▾ |         | -188.753 V | 47.995 V  |          | TH...   | 8.000 U        | 0.000     | 8.000         | 0.0... | 0.000      |
| 5 | IMAGE Standard ▾  |         | Infinity   | -         |          |         | 1.047          | 0.000     | 1.047         | 0.0... | 0.000      |

Figure 4.1 Lens data of the achromat (a).

The semi-diameter of the image is 1.047 mm and the semi-diameter of the object is 3.993 mm. The actual magnification is close to the ideal magnification 4x. The image space NA is 0.09942713 and the effective focal length (EFFL) is 42.53994 mm in the system data (Figure 4.2).

```

Effective Focal Length :      42.53994      (in air at system temperature and pressure)
Effective Focal Length :      42.53994      (in image space)
Back Focal Length      :      37.37151
Total Track           :      98.32226
Image Space F/#       :              5
Paraxial Working F/#  :      5.00389
Working F/#           :      5.004417
Image Space NA        :      0.09942713
Object Space NA       :      0.02501566
Stop Radius           :      4.253994
Paraxial Image Height :              1
Paraxial Magnification :     -0.2504296
Entrance Pupil Diameter :      8.507988
Entrance Pupil Position :              0
Exit Pupil Diameter   :      2738.621
Exit Pupil Position   :     -13703.73
Field Type            :      Paraxial Image height in Millimeters
Maximum Radial Field  :              1
Primary Wavelength [μm] :      0.5876
Angular Magnification :      0.003106781
Lens Units            :      Millimeters

```

Figure 4.2 System data of the achromat (a).

The layout of the system is in Figure 4.3.

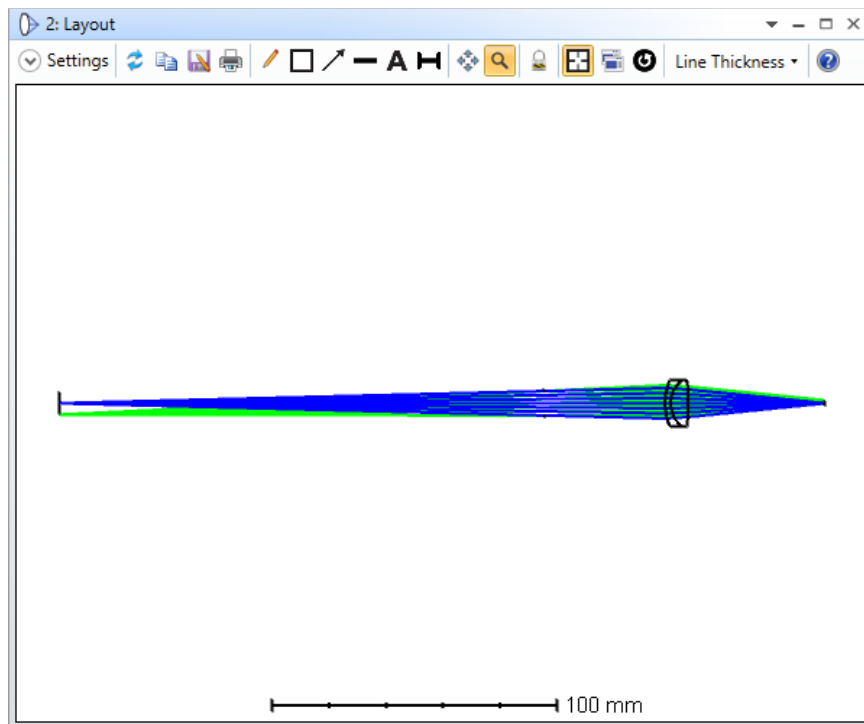


Figure 4.3 Layout of the achromat (a).

However, the chromatic focal shift (shown in Figure 4.4) is not right for an achromat. Two different colors can focus on the same focal point after passing through an achromat. It should be a “c” shape in the chromatic focal shift diagram [9].

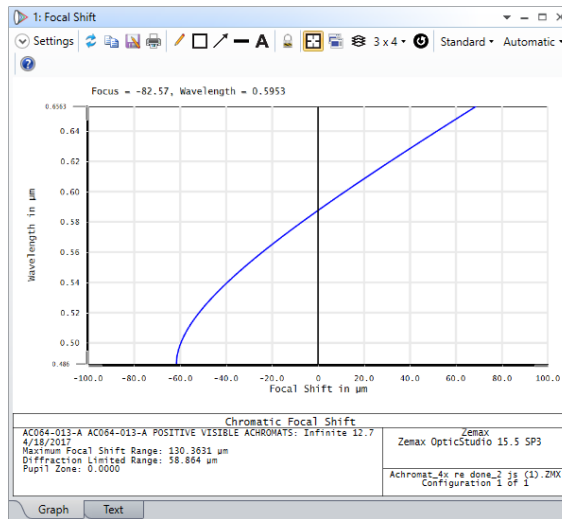


Figure 4.4 The chromatic focal shift of the achromat (a).

The Seidel diagram (Figure 4.5) also shows that the system has some spherical aberration and axial color.

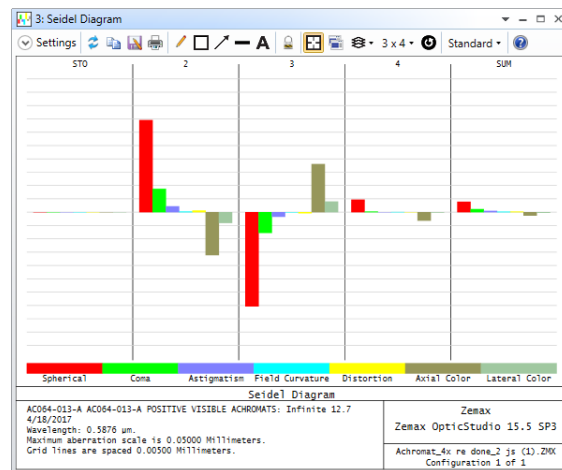


Figure 4.5 Seidel diagram of the achromat (a).

The merit function should be used to cancel some focal shift. The operand AXCL with the target of 0 is added in order to control the focal shift (Figure 4.6).

| Type   | Wave1  | Wave | Zo1  |      |      |      |  | Target | Weight  | Value | % Contrib |
|--------|--|------|------|------|------|------|--|--------|---------|-------|-----------|
| 1 RAID | 5  | 2    | 0... | 1... | 0... | 0... |  | 0.000  | 10.000  | 0.000 | 0.000     |
| 2 EFFL |  | 1    |      |      |      |      |  | 42.500 | 100.000 | 0.000 | 100.000   |
| 3 AXCL | 0  | 2    | 0... |      |      |      |  | 0.000  | 0.000   | 0.000 | 0.000     |
| 4 DMFS |  |      |      |      |      |      |  |        |         |       |           |
| 5 BLNK | Default merit function: RMS wavefront chief GQ 8 rings 10 arms |      |      |      |      |      |  |        |         |       |           |
| 6 BLNK | No default air thickness boundary constraints.                 |      |      |      |      |      |  |        |         |       |           |
| 7 BLNK | No default glass thickness boundary constraints.               |      |      |      |      |      |  |        |         |       |           |
| 8 BLNK | Operands for field 1.  |      |      |      |      |      |  |        |         |       |           |

Figure 4.6 Merit function of the achromat (a).

When the weight of an operand is higher than others, Zemax is more likely to meet the requirement of this operand when it is optimizing the system. If the AXCL has a weight of 100, the focal shift (Figure 4.7) is much better than before [10].

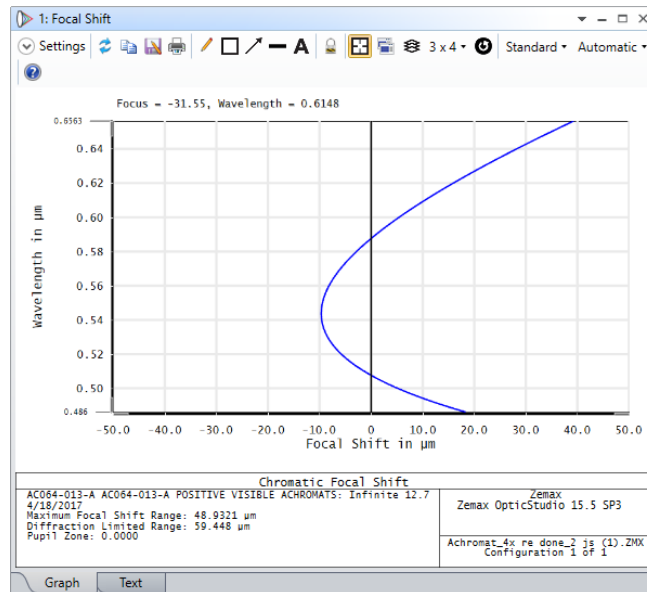


Figure 4.7 The chromatic focal shift of the achromat (b).

There is almost no axial color in the Seidel diagram (Figure 4.8).

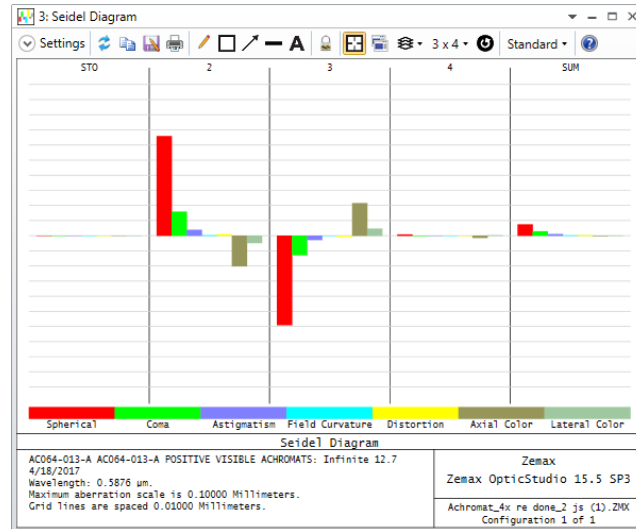


Figure 4.8 Seidel diagram of the achromat (b).

However, this system is not perfect as well. The image space NA is not as good as it was in the model before adding the AXCL operand (shown in Figure 4.9).

```

Effective Focal Length :      42.48014      (in air at system temperature and pressure)
Effective Focal Length :      42.48014      (in image space)
Back Focal Length      :      35.83925
Total Track            :      97.61677
Image Space F/#        :      5
Paraxial Working F/#   :      5.031219
Working F/#           :      5.029185
Image Space NA         :      0.09889234
Object Space NA        :      0.02498052
Stop Radius           :      4.248014
Paraxial Image Height  :      1
Paraxial Magnification :     -0.2514434
Entrance Pupil Diameter :      8.496028
Entrance Pupil Position :      0
Exit Pupil Diameter   :      342.1404
Exit Pupil Position   :     -1721.407
Field Type             :      Paraxial Image height in Millimeters
Maximum Radial Field   :      1
Primary Wavelength [ $\mu\text{m}$ ] :      0.5876
Angular Magnification  :      0.02483218
Lens Units             :      Millimeters
  
```

Figure 4.9 System data of the achromat (b).

The image NA is 0.9889234, which is less than the image NA in the last model.

The result may be different if the achromat has the convex lens in the front, by setting the thickness of the second surface as 6 mm and the thickness of the third surface as 2 mm. The materials are also exchanged. The layout of the system is in Figure 4.10.

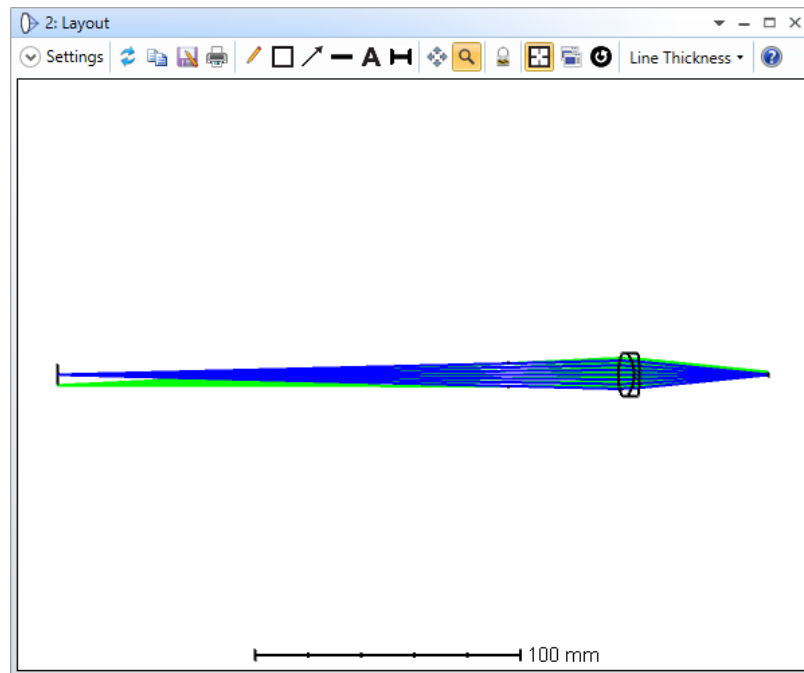


Figure 4.10 Layout of the achromat (c).

The radius of each surfaces is different from the models above (Figure 4.11).

|   | Surf.Type | Comment  | Radius    | Thickness | Material | Coating | Clear Semi-Dia | Chip Zone | Mech Semi-Dia | Conic  | TCE x 1E-6 |
|---|-----------|----------|-----------|-----------|----------|---------|----------------|-----------|---------------|--------|------------|
| 0 | OBJECT    | Standard | Infinity  | 170.000   |          |         | 3.996          | 0.000     | 3.996         | 0.0... | 0.000      |
| 1 | STOP      | Standard | Infinity  | 41.434 V  |          |         | 4.248          | 0.000     | 4.248         | 0.0... | 0.000      |
| 2 | (aper)    | Standard | 23.347 V  | 6.000     | BK7      | TH...   | 8.000 U        | 0.000     | 8.000         | 0.0... | -          |
| 3 | (aper)    | Standard | -14.431 V | 2.000     | F2       |         | 8.000 U        | 0.000     | 8.000         | 0.0... | -          |
| 4 | (aper)    | Standard | -69.790 V | 48.668 V  |          | TH...   | 8.000 U        | 0.000     | 8.000         | 0.0... | 0.000      |
| 5 | IMAGE     | Standard | Infinity  | -         |          |         | 1.044          | 0.000     | 1.044         | 0.0... | 0.000      |

Figure 4.11 Lens data of the achromat (c).

The focal shift is better than the last model (Figure 4.12).

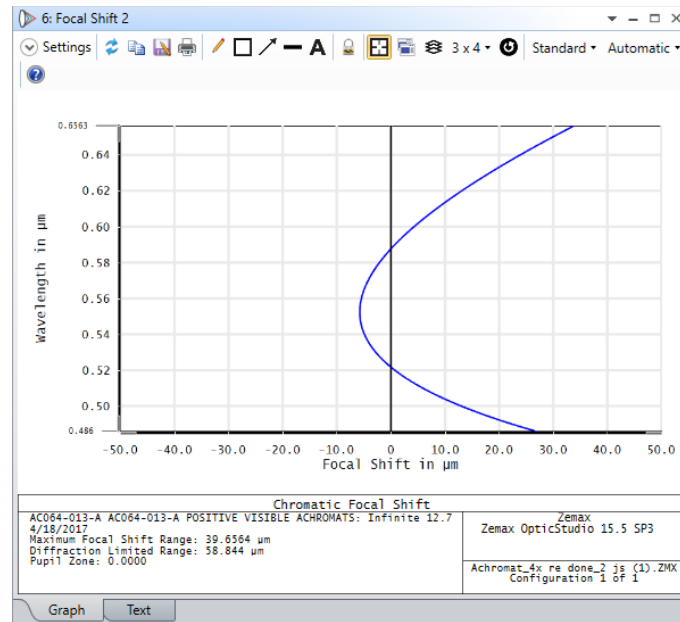


Figure 4.12 Focal shift of the achromat (c).

The spherical aberration is much smaller compared to other models as well based on the Seidel diagram (Figure 4.13).

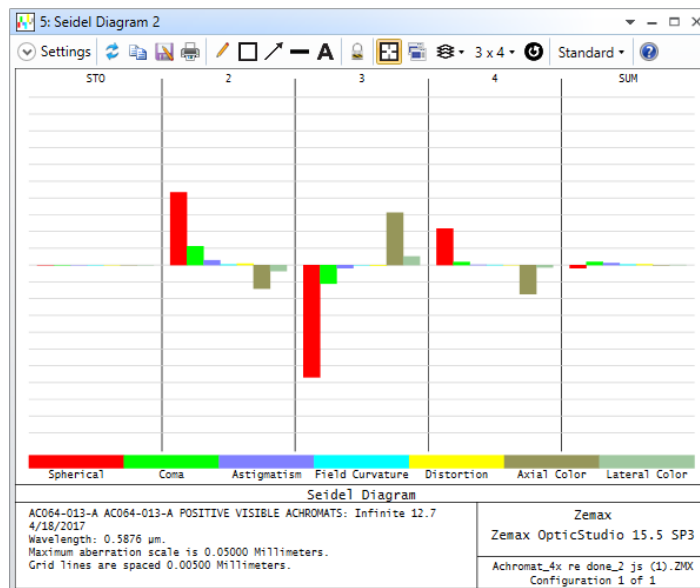


Figure 4.13 Seidel diagram of the achromat (c).

The image space NA is 0.09934623 (Figure 4.14). This system has a better image space NA than the models above.

|                         |   |                                      |   |
|-------------------------|---|--------------------------------------|---|
| Effective Focal Length  | : | 42.47539                             | (in air at system temperature and pressure) |
| Effective Focal Length  | : | 42.47539                             | (in image space)                            |
| Back Focal Length       | : | 37.93777                             |   |
| Total Track             | : | 98.10193                             |   |
| Image Space F/#         | : | 5                                    |   |
| Paraxial Working F/#    | : | 5.008006                             |   |
| Working F/#             | : | 5.003566                             |   |
| Image Space NA          | : | 0.09934623                           |   |
| Object Space NA         | : | 0.02497773                           |   |
| Stop Radius             | : | 4.247539                             |   |
| Paraxial Image Height   | : | 1                                    |   |
| Paraxial Magnification  | : | -0.2502553                           |   |
| Entrance Pupil Diameter | : | 8.495077                             |   |
| Entrance Pupil Position | : | 0                                    |   |
| Exit Pupil Diameter     | : | 1327.815                             |   |
| Exit Pupil Position     | : | -6649.807                            |   |
| Field Type              | : | Paraxial Image height in Millimeters |   |
| Maximum Radial Field    | : | 1                                    |   |
| Primary Wavelength [μm] | : | 0.5876                               |   |
| Angular Magnification   | : | 0.006397932                          |   |
| Lens Units              | : | Millimeters                          |   |

Figure 4.14 System data of the achromat (c).

In fact, the model above is the most common achromat type. The crown glass BK7 is in the front and the flint glass F2 is in the back. BK7 and F2 may not be the best solution for the achromat as long as other types of glass work better. The solve type of the materials can be changed to substitute. Zemax will search for the best material after using hammer optimization. For instance, BALKN3 and SF3 work better in this system. However, the materials, which are used in the objective lens may not be the best combination. The cost of the material is also a significant consideration when it comes to manufacture objectives.

The advantages and disadvantages of the three simulation models are summarized in Table 7, and the achromat (c) BK7-F2 model is the best among the three models in this chapter.

Table 7 Comparison of three achromatic objective models.

|                                 | <b>Advantages</b>  | <b>Disadvantages</b>                             |
|---------------------------------|--|--|
| <b>(a) F2-BK7</b>               | More accurate image space NA and<br>EFFL                                 | Not aplanatic<br>More chromatic<br>aberration    |
| <b>(b) F2-BK7<br/>with AXCL</b> | More accurate EFFL<br>Less chromatic aberration                          | Not aplanatic<br>Less accurate image space<br>NA |
| <b>(c) BK7-F2<br/>with AXCL</b> | Most accurate image space NA;<br>Less chromatic aberration;<br>Aplanatic |  |

Besides the comparison of the three achromat models, there is another comparison to do. Since there is a first order model in chapter 3 which supposed to be able to simulate different kinds of objectives, let's try to convert the achromat (c) model to a first order model and compare them as well.

From the cardinal points data (Figure 4.15), the actual front principal plane is at 42.203630 mm behind surface 1 and the distance between the rear principal plane and surface 5 is 53.205710 mm. The distance between surface 1 and 5 is 98.10193 mm based on the system data. Therefore, the distance between these two principal planes is  $98.10193 - 42.203630 - 53.205710 = 2.69259$  mm.

```
Starting surface : 1
Ending surface  : 5
Wavelength      : 0.587600
Orientation      : Y-Z
Lens units       : Millimeters
```

```
Object space positions are measured with respect to surface 1.
Image space positions are measured with respect to surface 5.
The index in both the object space and image space is considered.
```

|                       |   | Object Space | Image Space |
|-----------------------|---|--------------|-------------|
| Focal Length          | : | -42.475385   | 42.475385   |
| Focal Planes          | : | -0.271755    | -10.730325  |
| Principal Planes      | : | 42.203630    | -53.205710  |
| Anti-Principal Planes | : | -42.747140   | 31.745060   |
| Nodal Planes          | : | 42.203630    | -53.205710  |
| Anti-Nodal Planes     | : | -42.747140   | 31.745060   |

Figure 4.15 Cardinal points data of achromat (c).

Therefore, the lens data of the first order model can be set as Figure 4.16.

| Surf | Type   | Comment  | Radius   | Thickness | Material | Coating        | Semi-Diameter | Chip Zone | Mech Semi-Dia | Conic | TCE x 1E-6 | Focal Length |
|------|--------|----------|----------|-----------|----------|----------------|---------------|-----------|---------------|-------|------------|--------------|
| 0    | OBJECT | Standard | Infinity | 170.000   |          |                | 4.003         | 0.000     | 4.003         | 2.693 | 0.000      |              |
| 1    | STOP   | Standard | Front FP | Infinity  | 42.500   |                | 4.248         | 0.000     | 4.248         | 0.000 | 0.000      |              |
| 2    |        | Standard | Front PP | Infinity  | 0.337 P  |                | 6.310         | 0.000     | 6.310         | 0.000 | 0.000      |              |
| 3    |        | Paraxial |          | 0.337 P   |          |                | 6.327         | -         | -             |       | 0.000      | 0.337 P      |
| 4    |        | Standard |          | Infinity  | 0.337 P  |                | 0.016         | 0.000     | 0.016         | 0.000 | 0.000      |              |
| 5    |        | Paraxial |          |           | 0.337 P  |                | 6.294         | -         | -             |       | 0.000      | 0.337 P      |
| 6    |        | Standard |          | Infinity  | 0.337 P  |                | 6.310         | 0.000     | 6.310         | 0.000 | 0.000      |              |
| 7    |        | Paraxial |          |           | 0.337 P  |                | 6.327         | -         | -             |       | 0.000      | 0.337 P      |
| 8    |        | Standard |          | Infinity  | 0.337 P  |                | 0.016         | 0.000     | 0.016         | 0.000 | 0.000      |              |
| 9    |        | Paraxial | Rear PP  |           | 0.337 P  |                | 6.294         | -         | -             |       | 0.000      | 0.337 P      |
| 10   |        | Standard |          | 42.500    | 0.000    | 10000.00,0.0 M | 6.333         | 0.000     | 6.333         | 0.000 | 0.000      |              |
| 11   |        | Standard |          | 42.504    | 0.000    |                | 6.333         | 0.000     | 6.333         | 0.000 | 0.000      |              |
| 12   |        | Standard |          | Infinity  | 53.091 M |                | 6.382         | 0.000     | 6.382         | 0.000 | 0.000      |              |
| 13   | IMAGE  | Standard |          | Infinity  | -        |                | 1.006         | 0.000     | 1.006         | 0.000 | 0.000      |              |

Figure 4.16 Lens data of the converted first order model for achromat (c).

The achromat is converted as two principal planes (surface 2 to surface 9) and a thin lens (surface 10 and surface 11). The distance between surface 2 and surface 9 is 2.69259 mm, 3 standard surfaces and 4 thin lenses are equally separated between surface 2 and 9 to simulate the principal planes. The focal length of these 4 thin lenses is  $2.69259/8=0.336574$  mm. The thin lens which locates at the rear principal plane has a focal length of 42.5 mm by setting the radius of surface 10 as 42.5 mm and the radius of surface 11 as 42.504253 mm. The layout of the system is in Figure 4.17.

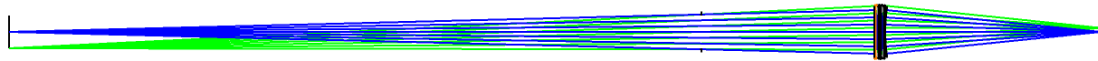


Figure 4.17 Layout of the converted first order model for achromat (c).

|                         |   |                                      |   |
|-------------------------|---|--------------------------------------|---|
| Effective Focal Length  | : | 42.47852                             | (in air at system temperature and pressure) |
| Effective Focal Length  | : | 42.47852                             | (in image space)                            |
| Back Focal Length       | : | 42.47852                             |   |
| Total Track             | : | 98.28403                             |   |
| Image Space F/#         | : | 5                                    |   |
| Paraxial Working F/#    | : | 4.999368                             |   |
| Working F/#             | : | 4.96977                              |   |
| Image Space NA          | : | 0.09951617                           |   |
| Object Space NA         | : | 0.02497957                           |   |
| Stop Radius             | : | 4.247852                             |   |
| Paraxial Image Height   | : | 1                                    |   |
| Paraxial Magnification  | : | -0.2498421                           |   |
| Entrance Pupil Diameter | : | 8.495704                             |   |
| Entrance Pupil Position | : | 0                                    |   |
| Exit Pupil Diameter     | : | 16796.7                              |   |
| Exit Pupil Position     | : | 83972.91                             |   |
| Field Type              | : | Paraxial Image height in Millimeters |   |
| Maximum Radial Field    | : | 1                                    |   |
| Primary Wavelength [μm] | : | 0.5875618                            |   |
| Angular Magnification   | : | -0.0005056906                        |   |
| Lens Units              | : | Millimeters                          |   |

Figure 4.18 System data of the converted first order model for achromat (c).

The effective focal length is 42.47852 mm and the image space NA is 0.09951617 based on the system data in Figure 4.18.

Table 8 Comparison between the actual achromat model and the first order model.

| <b>System data</b>             | <b>Actual achromat (c)</b> | <b>First order model of achromat (c)</b> |
|--------------------------------|----------------------------|--|
| <b>Effective focal length</b>  | 42.47539 mm                | 42.47852 mm                              |
| <b>Total Track</b>             | 98.10193 mm                | 98.28403 mm                              |
| <b>Working F/#</b>             | 5.003566                   | 4.96977                                  |
| <b>Image Space NA</b>          | 0.09934623                 | 0.09951617                               |
| <b>Paraxial Magnification</b>  | -0.2502553                 | -0.2498421                               |
| <b>Entrance Pupil Diameter</b> | 8.495077 mm                | 8.495704 mm                              |

The system data of the two models are close enough (shown in Table 8) to prove that the first order model can be used to simulate the 4x/ 0.1 achromatic objective lens.

## CHAPTER 5. CONCLUSION

In this thesis, an overview of microscope objectives is summarized in chapter 1 and 2, including a brief review of the microscope history and some specifications and characteristics of microscope objectives. Users can choose the objective they need after understanding the meaning of the markings written/ painted on the objective barrel. The characteristics determine the performance of the objective. There are two types of the objective: refractive and reflective. The most used are refractive objectives and include achromat, plan achromat, fluorite, plan fluorite and plan apochromat. Plan apochromat corrects field curvature as well as spherical and chromatic aberration. In chapter 3, three first order models are built to simulate an infinity corrected objective; the only known specifications are magnification and NA. The third model which has standard surfaces and principal planes is the best one to simulate an objective because it provides proper ray heights. The objective model is aplanatic as well. This model can simulate any kind of objective without knowing the surface radius or the materials. In chapter 4, three models are built and optimized in order to find out a better solution for a finite 4x/ 0.1 achromatic objective. The achromat, which has the convex lens in the front and the concave lens at the back, corrects more aberration than the one with a concave lens in the front. These models illustrate some steps of optical design and optimization.

## REFERENCES

- [1] Who invented the microscope? A complete microscope history. (2010). In *History-of-the-microscope.org*. Retrieved from <http://www.history-of-the-microscope.org/history-of-the-microscope-who-invented-the-microscope.php>
- [2] Michael W. Davidson. (2016). Microscope Objective Specifications. Retrieved from <https://www.microscopyu.com/microscopy-basics/microscope-objective-specifications>
- [3] Objective Specifications. (2016). In *Education in Microscopy and Digital Imaging*. Retrieved from <http://zeiss-campus.magnet.fsu.edu/tutorials/objectivecolorcoding/>
- [4] Abramowitz, M. & Friedman, M. M. (May, 2001). Microscope Objectives. *Current Protocols in Cytometry*. DOI: 10.1002/0471142956.cy0202s00.
- [5] Abramowitz, M., Davidson, M. W., and al. (2013). The Microscopy. Retrieved from <https://optiki.files.wordpress.com/2013/03/abramowitz-and-davidson-microscopy.pdf>
- [6] Abramowitz, M. (2003). *Microscope Basics and Beyond*. Melville, NY: Olympus America Inc.
- [7] Dokland, Terje; Ng, Mary Mah-Lee (2006). Techniques in microscopy for biomedical applications. *p. 22-30*. ISBN 981-256-434-9.
- [8] Zemax LLC. (2016). OpticStudio (v16.5). Retrieved from <http://www.zemax.com/os/opticstudio>.
- [9] Sparrold, S. (2014, Feb 12). *Zemax 10 – Designing an Achromat*. [Youtube Video]. Podcast retrieved from <https://www.youtube.com/watch?v=OvmnovIzzJ4>.
- [10] Sun, H. (2017). *Lens Design a Practical Guide*. Boca Taton, FL: Taylor & Francis Group, LLC.